

# In vitro ovarian cancer model based on three-dimensional agarose hydrogel

Journal of Tissue Engineering  
5: 2041731413520438  
© The Author(s) 2014  
Reprints and permissions:  
sagepub.co.uk/journalsPermissions.nav  
DOI: 10.1177/2041731413520438  
tej.sagepub.com



Guojie Xu<sup>1, 2</sup>, Fuqiang Yin<sup>3</sup>, Huayu Wu<sup>4</sup>, Xuefeng Hu<sup>1</sup>,  
Li Zheng<sup>2, 3</sup>, Jinming Zhao<sup>1, 2</sup>

## Abstract

To establish a typical tumor model of ovarian cancer which may be more representative and reliable than traditional monolayer culture and pellet, agarose was used as cell vehicle to engineering tumor. Selection of agarose is based on its successful application in tissue engineering with both amenable mechanical and biological properties. In this study, ovarian cancer cell line SKOV3 was encapsulated in agarose hydrogel with cell aggregates and two-dimensional culture as controls. In vitro cell proliferation was assessed by MTT and cell viability was examined at time points of 2, 4, and 6 days. The expression of tumor malignancy markers including matrix metalloproteinase 2, matrix metalloproteinase 9, hypoxia-inducible factor-1 $\alpha$ , and vascular endothelial growth factor-A was assessed by real-time polymerase chain reaction. The results showed that cells proliferated more rapidly in three-dimensional agarose culture than controls. Furthermore, upregulation of matrix metalloproteinase 9 and matrix metalloproteinase 2 activity and increased expression of vascular endothelial growth factor-A and hypoxia-inducible factor-1 $\alpha$  were shown in agarose-engineered tumors. All the evidences demonstrated that agarose may provide a more favorable environment for cancer cell growth, mimicking the in vivo environment for tumor generation. The novel in vitro tumor model may be useful for the further investigation of anticancer therapeutics.

## Keywords

Agarose, tumor engineering, ovarian cancer, tumor microenvironment

Received: 24 September 2013; accepted: 16 December 2013

## Introduction

Epithelial ovarian cancer accounts for 25%–30% of all the gynecologic cancers and has the highest mortality rate.<sup>1,2</sup> To improve the survival of patients, early cognition and treatment of ovarian cancer are imperative. As a prerequisite, a predictive and reproducible cancer model that could reliably translate preclinical results to efficacy in human patients should be developed.

As is well known, the communication between the cancer cell and tumor microenvironment that regulates various physiological processes such as cell differentiation, proliferation, and expression of various genes is essential for tumorigenesis.<sup>3,4</sup> Traditional two-dimensional (2D) model using monolayer culture can hardly recapitulate three-dimensional (3D) cell morphology and may distort cell–matrix interactions, as it can hardly provide biomimetic environment in which tumors reside.<sup>5–7</sup> Until recently, the biological significance and clinical relevance of tumor cells that grow in 3D environment were claimed, as evidenced by enhanced cell–cell interactions, intercellular adhesion,

and signaling between cells. Cell pellet culture is a kind of 3D models, but the loose structure may disintegrate cell communication.<sup>8</sup> In most studies, scaffold-based

<sup>1</sup>Osteopathy Ward, The First Affiliated Hospital, Guangxi Medical University, Nanning, Guangxi, China

<sup>2</sup>Research Center for Regenerative Medicine, Guangxi Medical University, Guangxi Medical University, Nanning, Guangxi, China

<sup>3</sup>The Medical and Scientific Research Center, Guangxi Medical University, Guangxi Medical University, Nanning, Guangxi, China

<sup>4</sup>Department of Cell Biology & Genetics, School of Premedical Sciences, Guangxi Medical University, Nanning, Guangxi, China

\* Fuqiang Yin contributed equally to this work.

## Corresponding authors:

Li Zheng, The Medical and Scientific Research Center, Guangxi Medical University, Nanning, Guangxi 530021, China.  
Email: zhengli224@163.com

Jinming Zhao, Osteopathy Ward, The First Affiliated Hospital, Guangxi Medical University, Nanning, Guangxi 530021, China.  
Email: zhaojinmin@126.com

tumor engineering is advantageous to model 3D tumor spheroids.<sup>9–15</sup> To guide the tumor development, selection of favorable scaffold is the key.<sup>16,17</sup>

In scaffold-based tumor engineering, research has focused on the development of bioresorbable scaffolds with both optimal mechanical properties and excellent biocompatibility. Natural and synthetic scaffolds have been widely adopted in tumor engineering. Natural scaffolds are mainly hydrogels made of natural materials or proteins like collagen type I, laminin, or hyaluronic acid.<sup>18</sup> However, these hydrogels were affected by a number of factors, including the source, cross-linking chemistry, temperature, pH, ionic strength, ion stoichiometry, as well as the monomer concentration.<sup>19–21</sup> Unlike these hydrogels, agarose is more stable. Agarose has broad utility in preclinical applications, such as substrate of choice in numerous biocompatibility tests including cytotoxicity, genotoxicity, mutagenesis, sensitivity, and subcutaneous implants; in gene therapy; and in drug delivery systems.<sup>5</sup> The size and stiffness of agarose can be adjusted according to the need of tumor engineering.<sup>22,23</sup> This may afford mechanical advantages to agarose to mimic the naturally stiff environment in which most tissue cells or tumor cells reside. On the other hand, agarose hydrogel can well support cell proliferation and maintain the phenotype *in vitro*, which has been well demonstrated in a great number of tissue engineering studies.<sup>23–39</sup> Most importantly, it can enhance the secretion of extracellular matrix (ECM) by supplying an appropriate environment for a stable cell phenotype.<sup>33</sup> Besides, it is easy to be reproducibly manufactured, convenient to be handled, and amenable to large-scale use. Although agarose is an excellent cell vehicle for tissue regeneration, few researches considered agarose as a potential candidate for 3D tumor model. Whether it would provide an amenable biocompatible 3D microenvironment for tumorigenesis is seldom investigated. Concerning its successful application in tissue engineering, we reasonably believe that agarose may facilitate tumor progression.

Based on the assumption that agarose may recapitulate the major cues provided by the tumor microenvironment, 3D *in vitro* model of ovarian cancer was constructed by encapsulating ovarian cancer cell line SKOV3 in agarose hydrogel in this study. Cell aggregates without scaffold were used as control. We also compared the 3D model with monolayer culture. Tumor malignancy was assessed by real-time polymerase chain reaction (PCR) analysis of key growth factors and metalloprotease concerning tumor growth. The aim of this study is to build a representative and reliable model for cancer research.

## Materials and methods

### Cell lines and culture

Cell line SKOV3 of the human epithelial ovarian serous adenocarcinoma derived from ascites fluid was purchased

from China Center for Type Culture Collection (CCTCC) and grown in RPMI 1640 (Gibco BRL, Gaithersburg, MD USA) 10% fetal bovine serum (FBS) (Hyclone, Logan, UT USA), 1% penicillin, and streptomycin (Solarbio, PEK, China) in atmosphere at 37°C and 5% CO<sub>2</sub>.

### Preparation of agarose hydrogels

Agarose was purchased from Sigma-Aldrich, St. Louis, USA. Hydrogel was prepared by dissolving agarose (2% wt) in aqueous solvent at the temperature of 90°C. Once the temperature of this solution is lowered to room temperature, gelation will occur.

### Cells packaged in 3D scaffold and cultured on 2D scaffold

Cells were harvested using 0.25% trypsin/ethylenediaminetetraacetic acid (EDTA) (Solarbio, China), counted, and then loaded in agarose scaffolds. Briefly, cells were suspended in 2% agarose with the cell density of 10<sup>7</sup> cells/100 µL. The agarose molds were allowed to gelation at 37°C for 10 min, and then transferred to 15 mL centrifuge tube containing medium of RPMI 1640, 10% FBS, 1% penicillin, and streptomycin. The tube was placed in incubator containing 5% CO<sub>2</sub> at 37°C. As control, cell aggregates (10<sup>7</sup> cells deposited at each tube bottom after centrifuge) were cultured with the same condition as that of experiment group. To compare 3D model with 2D model, cells in monolayer were also cultured for analysis. Culture media were changed every 2 days. Assays were performed at time points of 2, 4, and 6 days.

### Cell proliferation assay

At each time point, samples in all groups were incubated in 5 mg/mL 3-(4,5-dimethylthiazol-2-yl)-2,5-diphenyltetrazolium bromide (MTT) reagent for 4 h at 37°C, 5% CO<sub>2</sub> environment. After removal of the incubation medium, 1 mL dimethyl sulfoxide (DMSO) was added in each well to dissolve formazan pigment. Pellet and monolayer group were directly analyzed. For agarose group, the hydrogel was then smashed and centrifuged at 11,000 rpm to ensure the complete extraction of the formazan pigment by DMSO. The absorbance at 570 nm was recorded under a microplate reader (Bio-Rad 550, Hercules, CA, USA).

### Cell viability assay

Cell viability was examined by a Live/Dead cell assay kit (Invitrogen, Carlsbad, CA, USA) at days 2, 4, and 6. 1 µM calcein–acetomethoxy deriviate (AM) and 1 µM propidium iodide (PI) were added to the cell culture dish and incubated for 5 min at 37°C. The cells were visualized with laser scanning confocal microscope (Nikon A1, TYO, Japan).

**Table 1.** Genes and oligonucleotide primers used in PCR analysis.

Gene	Primer sequence (5' to 3')	Length (bp)	T <sub>m</sub> (°C)	GC (%)	Amplicon size (bp)
MMP-2	F:CGACCACAGCCAACTACGAT	20	60	55	224
	R:GTCAGGAGAGGCCCATAGA	20	60	60	
MMP-9	F:CGACGTCTTCCAGTACCGAG	20	60	60	220
	R:TTGTATCCGGCAAACCTGGCT	20	60	50	
HIF-1 $\alpha$	F:AGTGCTGACCCTGCACTCAAT	21	61	52	377
	R:GGGCTTGCGGAACTGCTTTC	20	61	60	
VEGF-A	F:TGCTGTCTTGGGTGCATTGG	20	60	55	163
	R:AGGGTCTCGATTGGATGGCAG	21	60	57	

PCR: polymerase chain reaction; MMP: matrix metalloproteinase; HIF: hypoxia-inducible factor; VEGF: vascular endothelial growth factor–A. F means forward primer and R means reversed primer.

### Cell morphological analysis

Samples in all groups were permeabilized using 0.5% Triton X-100 (Sigma-Aldrich), with 1% bovine serum albumin (BSA) (Santa Cruz Biotechnology, Inc., Santa Cruz, CA, USA) as a blocking buffer for 30 min at 37°C. Cells were stained for 30 min at room temperature with rhodamine phalloidin (Invitrogen), followed by Hoechst 33258 (Beyotime, MA, USA) for 5 min to visualize nuclei. Imaging was performed using scanning confocal microscope (Nikon A1).

### Gene expression analysis

The gene expression levels of matrix metalloproteinase 2 (MMP-2), MMP 9, hypoxia-inducible factor (HIF-1 $\alpha$ ), and vascular endothelial growth factor–A (VEGF-A) were measured using quantitative reverse transcription PCR (qRT-PCR). Total RNA was isolated using TRI Reagent Solution (Applied Biosystems, Carlsbad, CA, USA/Ambion, Austin, TX, USA) on days 2, 4, and 6. Next, 1 mg of total RNA was reverse-transcribed to complementary DNA (cDNA) using a Reverse Transcription System (Promega, Madison, WI, USA). Finally, an ABI 7300 Sequence Detection System (Applied Biosystems) was used to conduct qRT-PCR using TaqMan Universal PCR Master Mix and gene-specific TaqMan PCR primers (Applied Biosystems) (Table 1): MMP-2 (NM\_001127891.1), MMP-9 (NM\_004994.2), HIF-1 $\alpha$  (NM\_001530.3), and VEGF-A (NM\_001025366.2). Gene expression was normalized to glyceraldehyde 3-phosphate dehydrogenase (GAPDH) using the comparative threshold cycle ( $\Delta\Delta$ CT) method of quantification.<sup>40</sup> All experiments were performed with four technical replicates.

### Statistical analysis

Gene expression levels measured by qRT-PCR were analyzed for significance using an analysis of variance (ANOVA) test with a Tukey post hoc test;  $p < 0.05$  was considered significant, and  $p < 0.01$  and  $p < 0.001$  were also noted.

## Results

### Cells proliferation

As shown in Figure 1, the cell density in 3D agarose group was significantly higher than pellet, which was much higher than the 2D group at different time points. The results suggested that 3D agarose could better support cell growth than pellet and traditional 2D monolayer.

### Cell viability

As shown in Figure 2, 3D agarose constructs showed relatively uniform distributions of cells with viability greater than 95% at each time point. Cells in agarose scaffold displayed a spherical morphology that persisted throughout the culture period, in comparison with monolayer culture. In 3D agarose model, cell proliferation is obvious, as evidenced by increased amount of live cells over time. In comparison, pellet exhibited less obvious proliferation and more dead cells than agarose group. Due to limited space, the most notable cell death was shown in monolayer culture.

### Observation of cell morphology

As shown in Figure 3, the cells in 3D agarose and pellet culture developed a stellate, round morphology with disorganized nuclei, throughout the culture period. In contrast, cells were fusiform in 2D culture. As reflected by more cells and more notable cell growth, and more secreted matrix, agarose may better promote cell–matrix and cell–cell interactions than pellet and monolayer.

### Bioengineered tumor migration, hypoxic, and angiogenic gene expression profile

The markers of tumor malignancy include MMP-2, MMP-9, HIF-1 $\alpha$ , and VEGF-A, upregulation of which indicated promotion of an in vivo phenotype.<sup>2,25</sup> MMP-2 and MMP-9 were involved in invadopodia formation belonging to a family of 25 zinc-dependent endopeptidases that allow

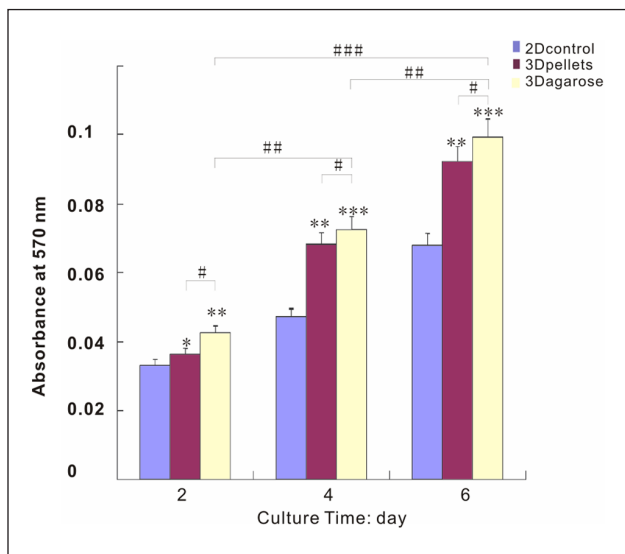


**Figure 1.** MTT was used to analyze cell proliferation in 3D and 2D cultures. The cell proliferation in 3D agarose was higher than pellets and 2D monolayer at 2, 4, and 6 days. 2D culture showed the lowest cell numbers among the groups. \*/#, \*\*\*/###, and \*\*\*/###/### denote  $p < 0.05$ ,  $p < 0.01$ , and  $p < 0.001$ , respectively. MTT: 3-(4,5-dimethylthiazol-2-yl)-2,5-diphenyltetrazolium bromide; 3D: three-dimensional; 2D: two-dimensional.

cells to both sense and remodel their environment by cleaving extracellular factors and matrix proteins.<sup>41</sup> MMP-9 and MMP-2 are considered to be two of the most important parameters for ECM degradation and metastasis.<sup>42,43</sup> As shown in Figure 4, MMP-2 and MMP-9 were significantly elevated in 3D agarose, compared with the pellet and 2D system. Instead, there is no change in MMPs' expression with time under 2D culture. The results suggested that compared to 2D culture and pellet, 3D agarose could better promote the growth of tumors by providing a biomimetic microenvironment that can enhance the behaviors of cell–cell and cell–matrix.

VEGF-A and HIF-1 $\alpha$  factors are associated with pre-vascularized stages of tumor progression.<sup>44</sup> HIF-1 $\alpha$  was a key marker for identifying hypoxia,<sup>44–46</sup> and VEGF-A gene was activated in direct response to the development of hypoxia and HIF-1 $\alpha$  expression.<sup>47</sup> VEGF-A is a potent endothelial survival factor (VEGF masks BNIP3-mediated apoptosis of hypoxic endothelial cells) which may antagonize angiostatin's anti-angiogenic effects.<sup>48</sup> In Figures 5 and 6, HIF-1 $\alpha$  and VEGF-A were continuously upregulated with culture time, with significantly higher expression in 3D agarose than in the pellet and 2D culture. The upregulation of the two genes indicated that the degree of hypoxia was increased more evidently in 3D agarose, which was in accordance with rapid cell growth. The results demonstrated that agarose enhanced cell proliferation resulting in limited space for cells and oxygen diffusion, just like natural tumor formation in vivo.

## Discussion

The goal of this study is to engineer a typical 3D model of ovarian cancer that may substitute traditional Petri dish culture. Agarose as cell vehicle was chosen as candidate for engineering 3D model, owing to its amenable mechanical and biological properties, convenience to be handled, and most importantly, its successful application in tissue engineering and drug delivery.

Superior to high-density cell pellet and 2D culture, agarose culture supported persistent cell proliferation and enhanced cell growth. Obviously, cell proliferation is not so marked in monolayer as in 3D culture and more cells died, which may be due to the limited space for cell growth. This suggested that 2D culture poorly represented in vivo physiological conditions of tumor, as tumor cells were often characterized by rapid proliferation. For 3D model, engineered tumor by using scaffold is preferable over cell aggregates, as evidenced by more evident cell proliferation and more live cells remained over time. The biocompatibility and 3D architecture of agarose hydrogel were advantageous in supporting cell adhesion and cell distribution. In contrast, the loose structure of pellet may distort cell attachment and cell distribution. The result was in agreement with the findings that the use of scaffold-based constructs leads to a better retainment of ECM than the use of pellet cultures alone.<sup>49</sup> Moreover, it is of significance to introduce appropriate scaffold in tumor engineering to create 3D environment that can encourage the native scenario where cells migrate through matrix to form clusters, that is, the precursors of a tumor.<sup>18</sup> Further investigation revealed that 3D agarose may provide a more favorable microenvironment mimicking the in vivo environment for tumorigenesis, as demonstrated by upregulated expression of differential growth factors relating tumor malignancy. MMP-2, MMP-9, and VEGF-A were taken as part of the most important parameters for degradation of ECM and tumor metastasis.<sup>3,4</sup> In our study, activities of MMP-2 and MMP-9 were significantly upregulated when cultured in 3D agarose as opposed to 2D and pellet. It has been suggested that a simple cross-linked hydrogel recapitulated the majority of the cues provided by the tumor microenvironment without addition of any growth factors.<sup>18</sup> Cell communication and signaling representative of the native in vivo scenario may be encouraged by agarose through the promotion of cell–cell and cell–matrix interactions. And with the increase in culture time, the interactions were enhanced, as shown by higher levels of those angiogenic genes at later stage of culture period. The results were in agreement with the consistent cell proliferation for agarose-engineered constructs.

As one of the characteristics that mark the pre-vascularized stages of solid tumor growth, hypoxia surrounding a necrotic core is crucial to the tumor progression. Especially, HIF-1 $\alpha$  expression-mediated activation of VEGF-A gene

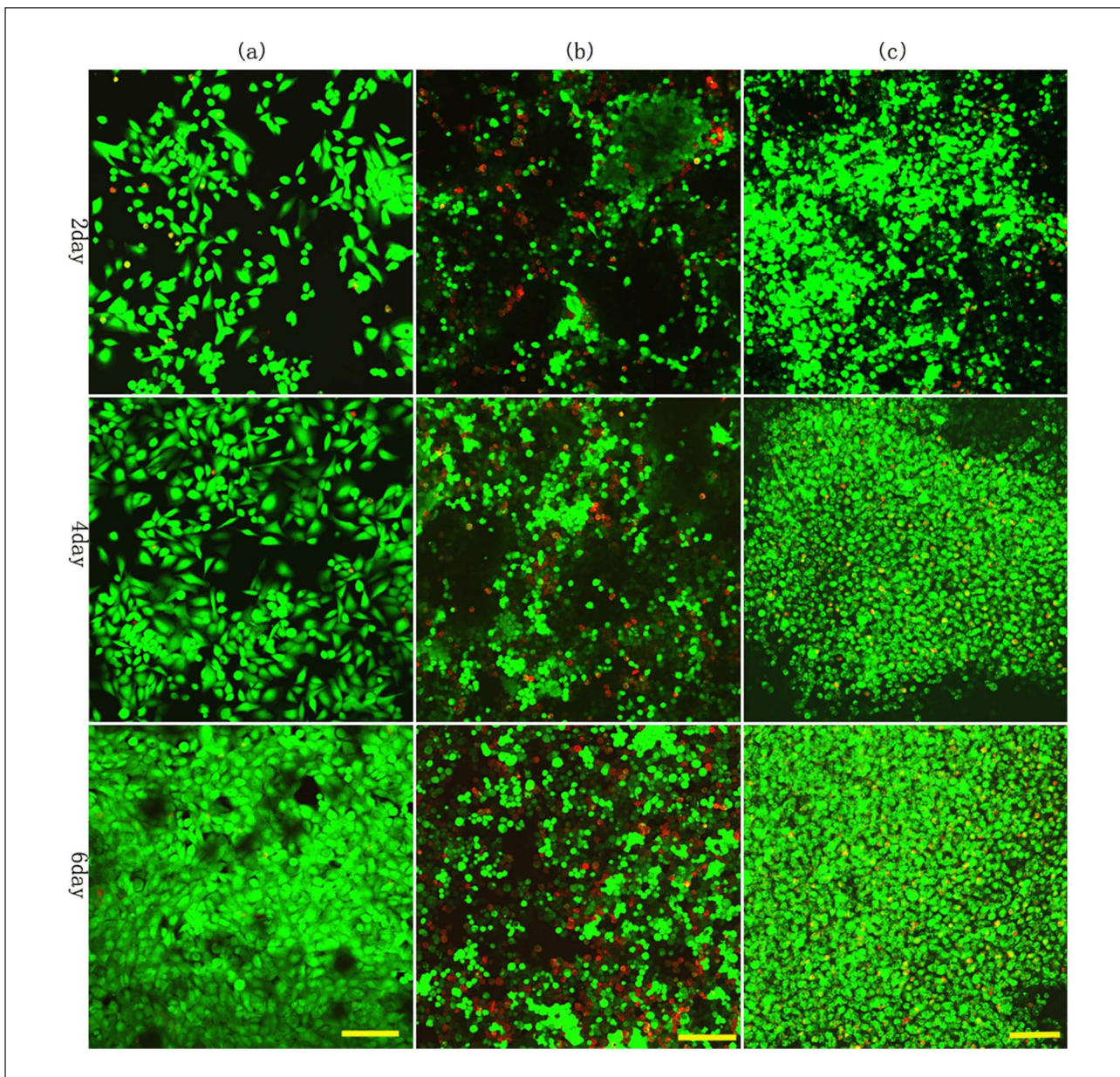


**Figure 2.** Cell viability in the agarose scaffold materials and in control groups visualized using confocal laser scanning microscopy and Live/Dead cell assay kit: (a) 2D control, (b) 3D control, and (c) 3D agarose. Cells in 3D agarose and pellets displayed a spherical morphology, while monolayer culture showed cells of fusiform morphology; proliferation in 3D agarose scaffolds is more rapid than the 3D control group. As limited by space, the most notable cell death was shown in monolayer culture. Scale bar is 100  $\mu\text{m}$ . 2D: two-dimensional; 3D: three-dimensional.

transcription is of importance for achieving a hypoxic microenvironment.<sup>48</sup> The presence of HIF-1 $\alpha$  reflects the hypoxic cellular response to being cultured in 3D.<sup>44</sup> Compared with monolayer and pellet that were in direct contact with oxygenated media, cells will have greater difficulty in obtaining oxygen and nutrients when confined within a 3D matrix. Higher expression of HIF-1 $\alpha$  in agarose tumor constructs than monolayer and pellet indicated that oxygen and nutrients were deficient for cells due to higher cell density. Especially at later stage when cells

formed clusters which could be observed by phalloidin staining, greater magnitude of HIF-1 $\alpha$  intensity exhibited revealing augmented degree of intracellular hypoxia. Representative of *in vivo* tumor progression, agarose-engineered tumor showed growing levels of VEGF-A in correlation with HIF-1 $\alpha$  upregulation. In monolayer and pellet, there were few changes in HIF-1 $\alpha$  over time as cells contact directly with oxygenated media.

In addition, pellet culture is not labor saving as agarose culture because each pellet was cultured individually at

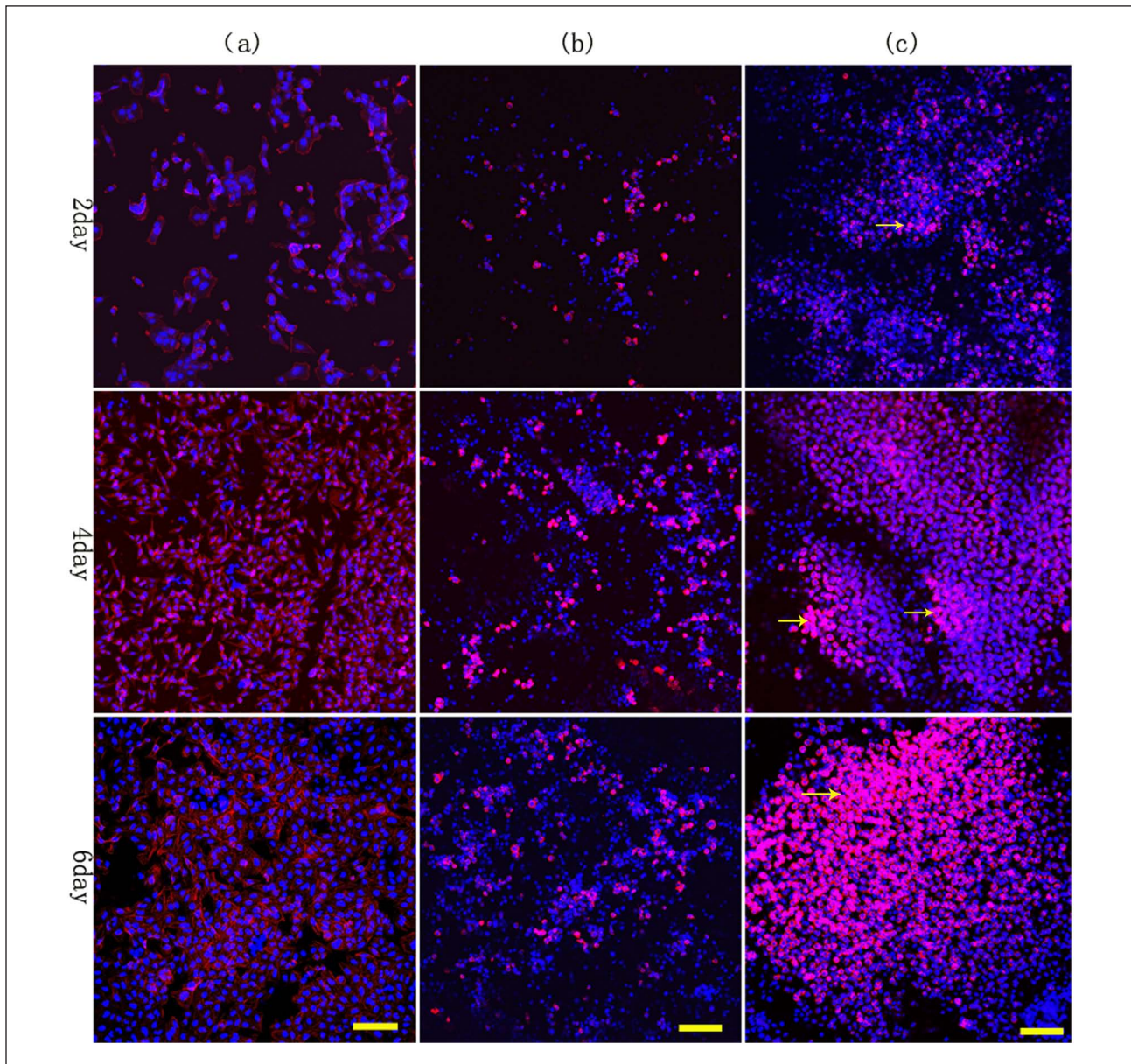


**Figure 3.** Morphology of ovarian cancer cells was observed after 2, 4, and 6, days of culture in agarose, pellets, and monolayer: (a) 2D control, (b) 3D control, and (c) 3D agarose. More cell numbers, more notable cell growth, as well as more matrix were presented in 3D agarose culture than in pellets culture. Obvious cell clusters was observed in 3D agarose. Scale bar is 100  $\mu\text{m}$ . Arrows indicate the clumps of cells in 3D agarose after 2, 4, and 6 days of culture. 2D: two-dimensional; 3D: three-dimensional.

one tube. Moreover, SKOV3 has weak pellet potential. Therefore, a suitable scaffold is imperative for the construction of *in vitro* tumor model. Based on the model, further study of the complex mechanisms of tumorigenesis may be more reliable.

## Conclusion

Referred from agarose-based tissue engineering with good performance, it was speculated that agarose may facilitate

tumor formation by providing tumor mimicking environment when applied to tumor engineering. In this study, results showed that agarose culture could well support tumor cell growth, with increased cell proliferation and cell viability compared to high-density pellet and monolayer culture. Further investigation revealed the enhanced tumor malignancy demonstrated by upregulated expression of hypoxic and pro-angiogenic factors. All the evidences revealed that agarose-engineered model of ovarian cancer may be representative and reliable as it can

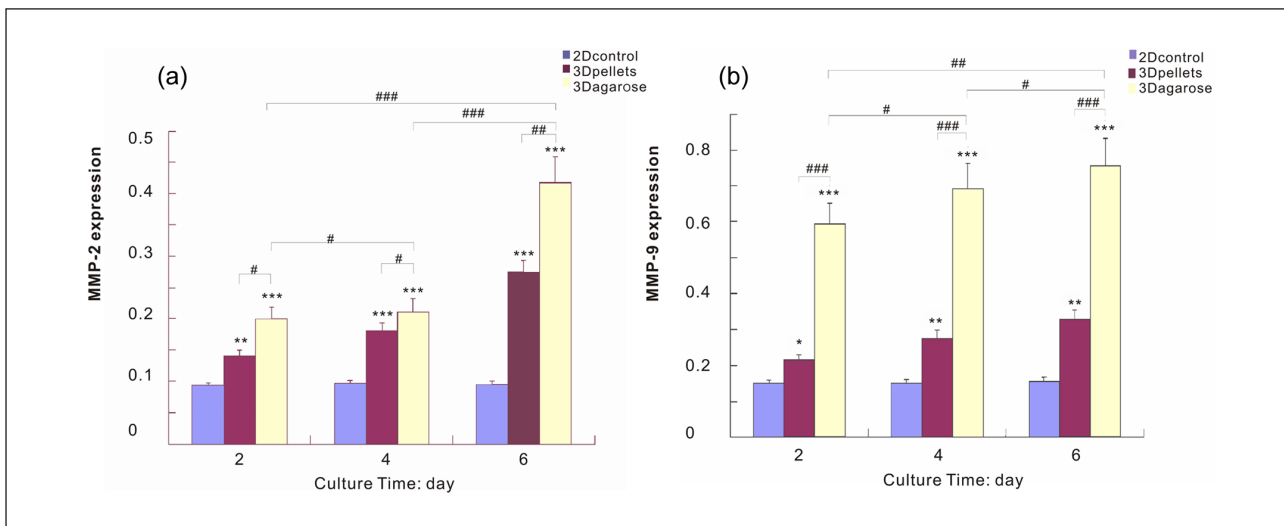


**Figure 4.** Quantitative RT-PCR was used to analyze the progression of MMP-2 and MMP-9 gene expression in both 3D and 2D cultures over a 6-day period: (a) MMP-2 and (b) MMP-9 were greatly upregulated in 3D agarose compared to the control groups, on days 2, 4, and 6. \*/#, \*\*/##, and \*\*\*/### denote  $p < 0.05$ ,  $p < 0.01$ , and  $p < 0.001$ , respectively.

RT-PCR: reverse transcription polymerase chain reaction; MMP: matrix metalloproteinase; 3D: three-dimensional; 2D: two-dimensional.

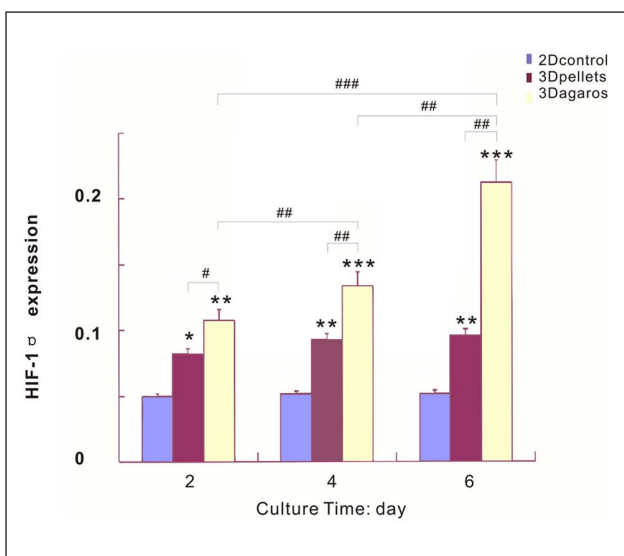


**Figure 5.** HIF-1 $\alpha$  gene expression was continuously increased over time in both 3D and pellets, in comparison to monolayer culture with little change. The expression of HIF-1 $\alpha$  was much higher in 3D agarose than in pellets and 2D culture. \*/#, \*\*/##, and \*\*\*/### denote  $p < 0.05$ ,  $p < 0.01$ , and  $p < 0.001$ , respectively.

HIF: hypoxia-inducible factor; 3D: three-dimensional; 2D: two-dimensional.

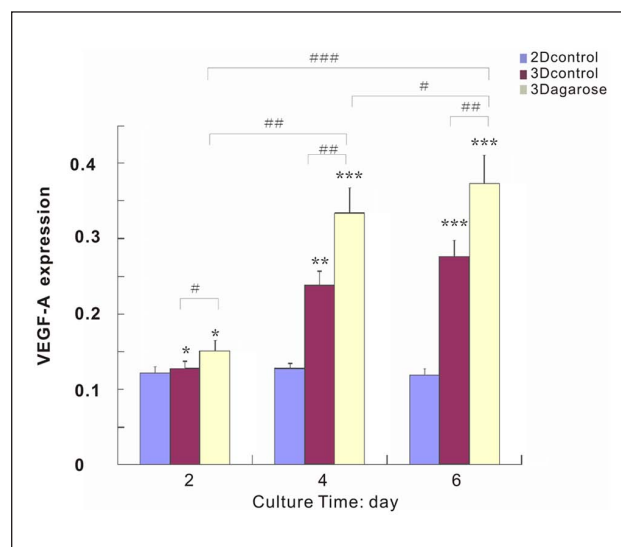


**Figure 6.** In correlation with HIF-1 $\alpha$ , VEGF-A exhibited sustained increase with time in both 3D and pellets. There is a little change in VEGF-A expression in monolayer culture. The expression of VEGF-A was much higher in 3D agarose than in pellets and 2D culture. \*/#, \*\*/##, and \*\*\*/### denote  $p < 0.05$ ,  $p < 0.01$ , and  $p < 0.001$ , respectively.

HIF: hypoxia-inducible factor; VEGF: vascular endothelial growth factor-A; 3D: three-dimensional; 2D: two-dimensional.

replicate the tumor microenvironment in vivo. This may facilitate further study of specific behaviors of ovarian cancer in vivo implicated in cancer development as well as screening anticancer drugs and chemoresistance.

### Declaration of conflicting interests

The authors declare that there is no conflict of interest.

### Funding

This work was financially supported by Guangxi Natural Science Foundation Program of China (Grant No. 2012GXNSFBA053114).

### References

1. Karabuk E, Kose MF, Hizli D, et al. Comparison of advanced stage mucinous epithelial ovarian cancer and

- serous epithelial ovarian cancer with regard to chemosensitivity and survival outcome: a matched case-control study. *J Gynecol Oncol* 2013; 24(2): 160–166.
2. Preston CC, Goode EL, Hartmann LC, et al. Immunity and immune suppression in human ovarian cancer. *Immunotherapy* 2011; 3(4): 539–556.
  3. Lukashev ME and Werb Z. ECM signalling: orchestrating cell behaviour and misbehaviour. *Trends Cell Biol* 1998; 8(11): 437–441.
  4. Bissell MJ and Radisky D. Putting tumours in context. *Nat Rev Cancer* 2001; 1(1): 46–54.
  5. Griffith LG and Swartz MA. Capturing complex 3D tissue physiology in vitro. *Nat Rev Mol Cell Biol* 2006; 7(3): 211–224.
  6. Yamada KM and Cukierman E. Modeling tissue morphogenesis and cancer in 3D. *Cell* 2007; 130(4): 601–610.
  7. Horning JL, Sahoo SK, Vijayaraghavalu S, et al. 3-D tumor model for in vitro evaluation of anticancer drugs. *Mol Pharm* 2008; 5(5): 849–862.
  8. Debnath J and Brugge JS. Modelling glandular epithelial cancers in three-dimensional cultures. *Nat Rev Cancer* 2005; 5(9): 675–688.
  9. Weigelt B and Bissell MJ. Unraveling the microenvironmental influences on the normal mammary gland and breast cancer. *Semin Cancer Biol* 2008; 18(5): 311–321.
  10. Grun B, Benjamin E, Sinclair J, et al. Three-dimensional in vitro cell biology models of ovarian and endometrial cancer. *Cell Prolif* 2009; 42(2): 219–228.
  11. Kievit FM, Florczyk SJ, Leung MC, et al. Chitosan–alginate 3D scaffolds as a mimic of the glioma tumor microenvironment. *Biomaterials* 2010; 31(22): 5903–5910.
  12. Hebner C, Weaver VM and Debnath J. Modeling morphogenesis and oncogenesis in three-dimensional breast epithelial cultures. *Annu Rev Pathol* 2008; 3: 313–339.
  13. Huttmacher DW, Horch RE, Loessner D, et al. Translating tissue engineering technology platforms into cancer research. *J Cell Mol Med* 2009; 13(8A): 1417–1427.
  14. Huttmacher DW, Loessner D, Rizzi S, et al. Can tissue engineering concepts advance tumor biology research? *Trends Biotechnol* 2010; 28(3): 125–133.
  15. Pampaloni F, Reynaud EG and Stelzer EH. The third dimension bridges the gap between cell culture and live tissue. *Nat Rev Mol Cell Biol* 2007; 8(10): 839–845.
  16. Huttmacher DW. Biomaterials offer cancer research the third dimension. *Nat Mater* 2010; 9(2): 90–93.
  17. Lutolf MP. Integration column: artificial ECM: expanding the cell biology toolbox in 3D. *Integr Biol (Camb)* 2009; 1(3): 235–241.
  18. Nyga A, Cheema U and Loizidou M. 3D tumour models: novel in vitro approaches to cancer studies. *J Cell Commun Signal* 2011; 5(3): 239–248.
  19. Engler AJ, Sen S, Sweeney HL, et al. Matrix elasticity directs stem cell lineage specification. *Cell* 2006; 126(4): 677–689.
  20. Trappmann B, Gautrot JE, Connelly JT, et al. Extracellular-matrix tethering regulates stem-cell fate. *Nat Mater* 2012; 11(7): 642–649.
  21. Witkowska-Zimny M, Walenko K, Walkiewicz AE, et al. Effect of substrate stiffness on differentiation of umbilical cord stem cells. *Acta Biochim Pol* 2012; 59(2): 261–264.
  22. Woolverton CJ, Fulton JA, Lopina ST, et al. Mimicking the natural tissue environment. *Tissue engineering and biodegradable equivalents: scientific and clinical applications*. New York: Marcel Dekker, 2002, pp. 43–75.
  23. Awad HA, Wickham MQ, Leddy HA, et al. Chondrogenic differentiation of adipose-derived adult stem cells in agarose, alginate, and gelatin scaffolds. *Biomaterials* 2004; 25(16): 3211–3222.
  24. Dolznig H, Rupp C, Puri C, et al. Modeling colon adenocarcinomas in vitro: a 3D co-culture system induces cancer-relevant pathways upon tumor cell and stromal fibroblast interaction. *Am J Pathol* 2011; 179(1): 487–501.
  25. Liu Y, Shu XZ and Prestwich GD. Tumor engineering: orthotopic cancer models in mice using cell-loaded, injectable, cross-linked hyaluronan-derived hydrogels. *Tissue Eng* 2007; 13(5): 1091–1101.
  26. Fischbach C, Chen R, Matsumoto T, et al. Engineering tumors with 3D scaffolds. *Nat Methods* 2007; 4(10): 855–860.
  27. Lutolf MP. Biomaterials: spotlight on hydrogels. *Nat Mater* 2009; 8(6): 451–453.
  28. Loessner D, Stok KS, Lutolf MP, et al. Bioengineered 3D platform to explore cell–ECM interactions and drug resistance of epithelial ovarian cancer cells. *Biomaterials* 2010; 31(32): 8494–8506.
  29. Ahearn M and Kelly DJ. A comparison of fibrin, agarose and gellan gum hydrogels as carriers of stem cells and growth factor delivery microspheres for cartilage regeneration. *Biomed Mater* 2013; 8(3): 035004.
  30. Hunt NC and Grover LM. Cell encapsulation using biopolymer gels for regenerative medicine. *Biotechnol Lett* 2010; 32(6): 733–742.
  31. Scarano A, Carinci F and Piattelli A. Lip augmentation with a new filler (agarose gel): a 3-year follow-up study. *Oral Surg Oral Med Oral Pathol Oral Radiol Endod* 2009; 108(2): e11–e15.
  32. Marczylo T, Arimoto-Kobayashi S and Hayatsu H. Protection against Trp-P-2 mutagenicity by purpurin: mechanism of in vitro antimutagenesis. *Mutagenesis* 2000; 15(3): 223–228.
  33. Hoffman BE, Newman-Tarr TM, Gibbard A, et al. Development and characterization of a human articular cartilage-derived chondrocyte cell line that retains chondrocyte phenotype. *J Cell Physiol* 2010; 222(3): 695–702.
  34. Erickson IE, Huang AH, Chung C, et al. Differential maturation and structure–function relationships in mesenchymal stem cell- and chondrocyte-seeded hydrogels. *Tissue Eng Part A* 2009; 15(5): 1041–1052.
  35. Kisiday JD, Kopesky PW, Evans CH, et al. Evaluation of adult equine bone marrow- and adipose-derived progenitor cell chondrogenesis in hydrogel cultures. *J Orthop Res* 2008; 26(3): 322–331.
  36. Sheehy EJ, Buckley CT and Kelly DJ. Chondrocytes and bone marrow-derived mesenchymal stem cells undergoing chondrogenesis in agarose hydrogels of solid and channelled architectures respond differentially to dynamic culture conditions. *J Tissue Eng Regen Med* 2011; 5(9): 747–758.
  37. Schwarz C, Leicht U, Drosse I, et al. Characterization of adipose-derived equine and canine mesenchymal stem cells after incubation in agarose-hydrogel. *Vet Res Commun* 2011; 35(8): 487–499.



38. Gadjanski I, Yodmuang S, Spiller K, et al. Supplementation of exogenous ATP enhances mechanical properties of 3D cell-agarose constructs for cartilage tissue engineering. *Tissue Eng Part A* 2013; 19: 2188–2200.
39. Varoni E, Tschon M, Palazzo B, et al. Agarose gel as bio-material or scaffold for implantation surgery: characterization, histological and histomorphometric study on soft tissue response. *Connect Tissue Res* 2012; 53(6): 548–554.
40. Schmittgen TD and Livak KJ. Analyzing real-time PCR data by the comparative CT method. *Nat Protoc* 2008; 3(6): 1101–1108.
41. Egeblad M and Werb Z. New functions for the matrix metalloproteinases in cancer progression. *Nat Rev Cancer* 2002; 2(3): 161–174.
42. Wang S, Li E, Gao Y, et al. Study on invadopodia formation for lung carcinoma invasion with a microfluidic 3D culture device. *PLoS One* 2013; 8(2): e56448.
43. Godugu C, Patel AR, Desai U, et al. AlgiMatrix™ based 3D cell culture system as an in-vitro tumor model for anticancer studies. *PLoS One* 2013; 8(1): e53708.
44. Szot CS, Buchanan CF, Freeman JW, et al. 3D in vitro bioengineered tumors based on collagen I hydrogels. *Biomaterials* 2011; 32(31): 7905–7912.
45. Zhou J, Schmid T, Schnitzer S, et al. Tumor hypoxia and cancer progression. *Cancer Lett* 2006; 237(1): 10–21.
46. Brahimi-Horn MC, Chiche J and Pouyssegur J. Hypoxia and cancer. *J Mol Med (Berl)* 2007; 85(12): 1301–1307.
47. Radziwon-Balicka A, Ramer C, Moncada de la Rosa C, et al. Angiostatin inhibits endothelial MMP-2 and MMP-14 expression: a hypoxia specific mechanism of action. *Vascul Pharmacol* 2013; 58(4): 280–291.
48. Costa A, Coradini D, Carrassi A, et al. Re: levels of hypoxia-inducible factor-1alpha during breast carcinogenesis. *J Natl Cancer Inst* 2001; 93(15): 1175–1177.
49. Schuurman W, Harimulyo E, Gawlitta D, et al. Three-dimensional assembly of tissue-engineered cartilage constructs results in cartilaginous tissue formation without retention of zonal characteristics. *J Tissue Eng Regen Med*. Epub ahead of print 18 April 2013. DOI: 10.1002/term.1726.